



# Application of Fractional Order Cascade Control to a Brake-By-Wire Actuator for Sport Motorcycles

Abhilash K. S<sup>1</sup>, Krishnapriya T Nair<sup>2</sup>

PG Scholar, ECE, Rajadhani Institute of Engineering & Technology, Trivandrum, India<sup>1</sup>

Assistant Professor, ECE, Rajadhani Institute of Engineering & Technology, Trivandrum, India<sup>2</sup>

**Abstract:** Fractional Order cascade control architecture to a brake-by-wire system which adapts the suitable controlling actions on breaking system for motor racing applications is described. An electromechanical actuator consisting of an electric motor, a transmission, a master cylinder, and a traditional hydraulic brake (pipe and calliper) are the consisting components of the system. A mathematical model of the system is derived and a fractional order cascade control is proposed. System consisting of two zones, dead zone and operative zone which are correspondingly the inner loop as well as outer of the controller. The inner loop is a position controller and outer a pressure controller. The outer loop features an adaptation mechanism to cope with the nonlinearities of the position–pressure relationship. The stability and robustness of the system are proven.

**Index Terms:** Actuator control, adaptive control, automotive, brake-by-wire (BBW), nonlinear control.

## I. INTRODUCTION

Vehicles performance not only the two wheeler but also four wheelers depends on a number of factors such as engine torque, type of fuel used, suspension, type of tyres used, breaking system etc. Among these factors the stability of the vehicle largely depends on breaking system. There are many a variety of breaking systems are being used in auto mobile industries. The ability of smoothly and precisely applying a desired braking torque is the basis of a safe braking system. The technological solutions which were proposed includes a variety of types such as the electrohydraulic one (EHB) is based on a hydraulic system, which is activated by an electric motor controlled by an electronic unit [8]-[11]. In electromechanical brake (EMB) there is an electric motor as actuator that provides the braking torque [12]-[14]. A particular EMB technology is known as wedge brake, where an electric motor controls the force on a wedge that pushes backward and forward the braking pads [15],[16].

A modified EHB with an electromechanical actuator that pushes backward and forward the piston of a master cylinder connected to a traditional hydraulic brake. As compared to EMB, this one has the advantage to keep the usual hydraulic layout unaltered but adding just the actuator. Thus weight, space, and cost are saved. The control problem is made nontrivial by the nonlinearities of the system due to friction, presence of the brake fluid reservoir, temperature variation, and oil compressibility and by the very demanding performance specifications. A disc brake is a type of brake that uses callipers to squeeze pairs of pads against a disc in order to create friction that retards the rotation of a shaft, such as

a vehicle axle, either to reduce its rotational speed or to hold it stationary. The rotating energy is converted into waste heat which must be dispersed. Hydraulic disc brakes are most commonly used form of brake for motor vehicles but the principles of a disc brake are applicable to almost any rotating shaft. Compared to drum brakes, disc brakes offer better stopping performance because the disc is more readily cooled. Also discs are less prone to the brake fade caused when brake components overheat. During riding, they are stabilized mainly by two mechanisms. Both stabilizing effects require a possible increase in side force. They must not work with sliding wheels, which happens on slippery surface. In the event of a locking front wheel, the motorcycle becomes kinematically unstable. A coupled yawing and rolling motion is induced that lets the motorcycle tumble in fractions of seconds. For technological constraints, at the end of the braking event the master cylinder piston must retract before the brake reservoir inlet so that a proper fluid compensation can be achieved. This introduces a nonlinearity in the system to be controlled.

Furthermore, the control law must be robust to the so-called knock-off. In racing applications, at times, the brake disk pushes back the pads at the end of the braking event. This leads to a variation in the position-pressure characteristic: during the following braking action, the master cylinder must move further than in the previous one. Then, after this anomalous braking event, the system returns to the normal behaviour. This happens in traditional brake too. Professional pilots feel the knock-off from the return force on the lever, and once detected, they



compensate it by pressing the brake lever more the closed-loop response with a direct pressure controller shows a big overshoot that prevents its usage in this application. The issue is addressed by simply avoiding to completely retract the piston. In this way, a good pressure tracking performance is achieved at the cost of the risk of not compensating fluid volume changes. Moreover, a small pressure is always applied to the brake pads: This causes a loss of energy and a continuous brake pad wear. In and, a hybrid position pressure switching control strategy has been proposed, in this way, through the position control, it is possible to compensate the fluid volume variation at the end of each braking event. The main problem of such an architecture is that in the first phase of the braking action when the position controller is enabled the pressure is not directly controlled. So, if there is a small error in the identified position–pressure map, the control performances are affected. Moreover, the architecture proposed in suffers from robustness issues. the aforementioned shortcomings are addressed by an adaptive cascade control architecture, which guarantees the required performance and improves robustness with respect to external disturbances. In this paper, the aforementioned shortcomings are addressed by an adaptive cascade control architecture, which guarantees the required performance and improves robustness with respect to external disturbances. Also, experimental results that prove the effectiveness of the control law are presented.

TABLE I GENERAL SPECIFICATIONS OF ELECTROMECHANICAL BBW ACTUATOR (DC MOTOR, TRANSMISSION AND MECHANICAL FRAME)

Weight	950	G
Height	42	mm
Length	105	mm
Width	75	mm
Motor Power	200	W

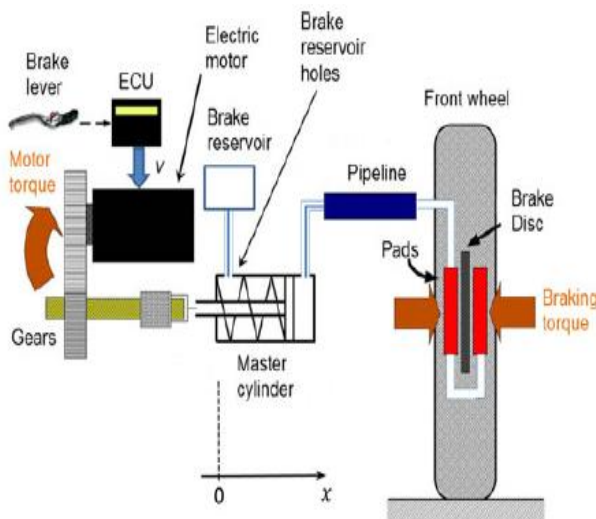


Fig 1 Schematic representation of the BBW system

II. SYSTEM DESCRIPTION

The system that we here considering is encompassed with an electromechanical actuator which is mechanically connected to a traditional hydraulic brake. The general specifications of BBW actuator are listed in Table I and schematic representation of the system is depicted in Fig.1.

The main components in figure are.

- 1) Brake lever: Pressure applied by the pilot which we considered as reference pressure is gathered from here.
- 2) BBW actuator: It consists of an electronic control unit which controls a dc motor that moves the master cylinder forward and backward through a mechanical transmission. The electronic board has a power bridge able to apply a voltage  $v$  on the motor clamps. The motor control is done through a current loop with a 100 – Hz bandwidth. The motor spinning is transformed into a linear movement by means of a mechanical transmission. There is a return spring that pushes the master cylinder backwards when no force is applied.
- 3) Hydraulic brake: The movement of the piston in master cylinder will varies the pressure in the hydraulic pump that, through the pipe, is transmitted to the brake calliper. The brake reservoir is an important part of this subsystem: at the end of each braking event, the master cylinder piston must retract before the brake reservoir holes. By way of which, the system compensates fluid volume variation due to temperature and brake pad wear.
- 4) Mechanical brake: According to the increment pressure in the brake calliper, the brake pads push against the brake disk through which the braking torque is generated.

III. MODELING OF SYSTEM

From the general specification of BBW actuator, the complete mathematical model can be derived [17] [18]. This study is focusing on a controller oriented model generation and its linearization in different working pointes. So we are consisting a number of assumptions for the ease of modelling the proposed system.

The assumptions are:

- 1) The motor current loop, which has the magnitude faster than the pressure dynamics so the electrical dynamics can be discarded. Therefore, the current is considered as the control variable;
- 2) Pressure in brake calliper and the pressure in the master cylinder are the same. Here, we are neglecting the pressure wave propagation dynamics
- 3) Fluid volume in the system is considered to be not varied by master cylinder position changes;
- 4) Static Coulomb friction is not considered. This can be done if a dithering signal is applied to the control variable ([18]–[20]) or if a suitable friction compensation technique is applied ([21]–[23]). With this assumption, we consider just the viscous friction contribution. It is then possible to derive a second-order control-oriented model.



$$M_{eq}\ddot{x} + K_{damp}\dot{x} + K_{spring}x + p(x)A_{mc} = iQ_{eq} \quad (1)$$

where

- 1)  $M_{eq}\ddot{x}$  is the mechanical inertial force and it can be represented as  $M_{eq} = M_{pist} + J_{mot}/K^2$  Where  $M_{pist}$  is the master cylinder piston mass,  $J_{mot}$  is the motor moment of inertia, and  $K$  is the transmission ratio;
- 2)  $K_{damp}\dot{x}$  is the damping force (due to viscous friction) and in general, it is unknown;
- 3)  $K_{spring}x$  represents the return spring force;
- 4)  $p(x)A_{mc}$  represents the return force due to the pressure in the master cylinder;
- 5)  $iQ_{eq}$  represents the equivalent force applied to the master cylinder piston by the motor and can be computed as  $K_T/K$ , where  $K_T$  is the motor torque constant.

TABLE II BBW COMPONENTS PHYSICAL PARAMETERS

$M_{pist}$	$10^{-3}$	kg
$J_{mo}$	$1.371 \cdot 10^{-5}$	$\text{Kg/m}^2$
$A_{mc}$	$1.13 \cdot 10^{-4}$	$\text{M}^2$
$KT$	0.0168	Nm/A
$K$	$0.3036 \cdot 10^3$	m/rad
$K_{spring}$	3000	N/m

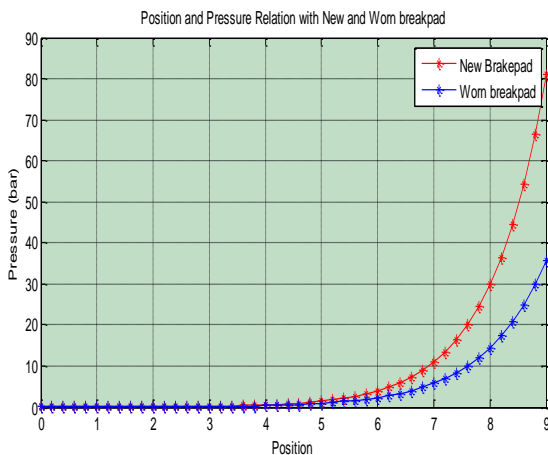


Fig. 2. Master cylinder position and pressure relationship with new and wore braking pads.

The model parameters are listed Table II. Note that they can be found from the BBW physical components, the only unknown parameter is  $K_{damp}$ . To model the relationship between position and pressure, we exploit the quasi-static experimental response of the system when an increasing current ramp followed by a decreasing one is applied, depicted in Fig. 2 (0A  $\rightarrow$  10A in 30 s, then 10A  $\rightarrow$  0A in 30 s). Which is a nonlinear static map. The position–pressure map is divided in two different zones (see Fig. 2): the dead zone and the operative zone respectively. Dead zone; where the master cylinder is before the brake reservoir, the piston moves with no pressure variation. The dead zone is not affected by temperature and brake pad wear. The second part of the

position–pressure curve is the operative zone; where the master cylinder is after the brake reservoir and a position increment corresponds to every pressure increment. This part of the position–pressure curve is strongly affected by temperature as well as brake pads wear. Note that the position–pressure map depicted in Fig. 2 presents a hysteresis. The average curve is considered for modelling purpose. The position–pressure curve introduces a time varying nonlinearity in the model (1), as it changes with temperature and pads wear. The linearized model allows for a quantification of the effect of the nonlinearity. Two different dynamics are analysed: the current-to-position dynamics and the current-to-pressure one.

Transfer function between current and position

$$G_x(S) = \frac{Q_{eq}}{(M_{eq} s^2 + K_{damp} s + p'(x)A_{mc})} \quad (2)$$

Transfer function between current and pressure

$$G_p(S) = \frac{(Q_{eq} p')}{(M_{eq} s^2 + K_{damp} s + p'(x)A_{mc})} \quad (3)$$

Where

$$p' = \left[ \frac{\partial p(x)}{\partial x} \right] \text{ at } x=x' \quad (4)$$

#### IV. CONTROL SYSTEM DESIGN

The control architecture is designed from the analysis of transfer function. While considering control architecture the dead zone must be considered (where a position controller is strictly needed), with different working points and with variations in the position–pressure map. Exploiting the fact that the position transfer functions are working point independent above a certain frequency, a specifically tuned linear position controller could make the closed loop robust with respect to the working point. Furthermore, an outer pressure loop is needed: in fact, the position–pressure map is time varying due to temperature and pads wear; so adopting just a position control would not be precise in terms of pressure tracking. These considerations lead to a position–pressure cascade control architecture (see Fig. 3)

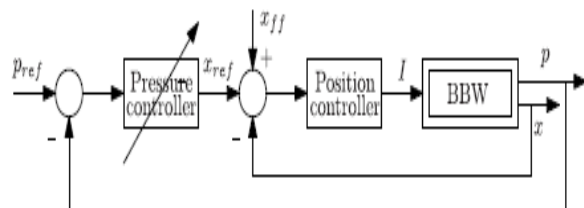


Fig 3 Position–pressure cascade control

##### A. Position Loop

The position loop is designed such that it must be able to track the reference with a closed-loop bandwidth around



50 Hz. For this the current-to-position model identification is performed around different working points. The system is maintained around mean  $x$  by means of a 1-Hz bandwidth position controller. The excitation signal is multifrequency sinusoidal current added into the loop as a load disturbance. The excitation signal frequency ranges from 10 to 200 Hz; this is consistent with the goal that we want to achieve. In the identification process since the closed-loop bandwidth is low compared to the excitation signal frequency, the control action and the excitation signal are decoupled in frequency. The same process is done maintaining the system around different working points, for each of them; the input (current) and the output (the position) are collected.

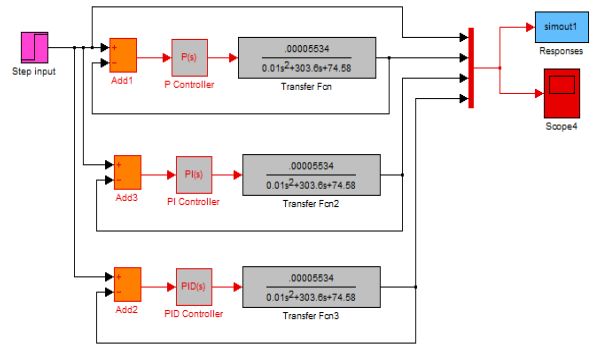


Fig 4: Simulink block diagram to find out closed loop response of current vs pressure.

**B. Pressure Loop**

The final control objective is pressure tracking and since the position–pressure relationship has a hysteresis and it is time varying, a standalone position loop is not enough, a pressure loop is required. The pressure loop must deal with the position– pressure nonlinearity depicted in Fig. 2 and it has to provide the same tracking performance under every condition. Since in the dead zone the pressure growth is negligible, the pressure controller will be designed to work in the operative zone. To cope with the presence of the dead zone, however, a supervising finite state machine is presented, that guarantees the proper controller working throughout the entire position–pressure map.

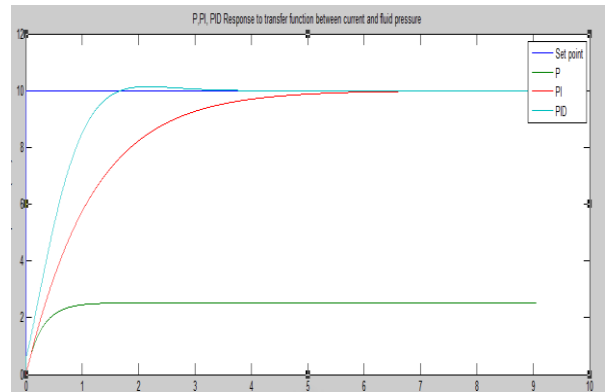


Fig 5: Closed loop response of current vs pressure

When designing the pressure controller in the cascade architecture, the control variable of interest is the reference position. The reference position  $\rightarrow$  pressure transfer function is, therefore, identified. The identification scheme adopted exploits the position controller designed in the previous subsection: a multifrequency reference position is injected; note that its average value establishes the working point where the identification is performed. Collecting the system input (reference position), together with the output (the pressure), a transfer function in each working point can be computed from the input/output cross power spectral density (solid lines in Fig. 6)

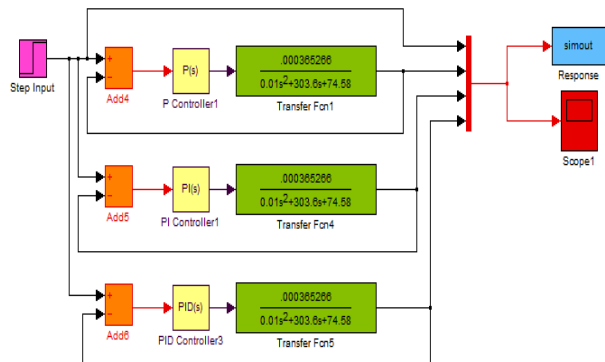


Fig 6: Simulink block diagram to find out closed loop response of current vs position

**C. Designing of controllers**

**CURRENT TO PRESSURE AND CURRENT TO POSITION**

For designing the controller for current to pressure loop Ziegler –Nichols Tuning method has chosen. Among the two methods consisting of open loop response method and closed loop response method, open loop response method which is comparatively less complicated and ease in calculation had chosen.

**OPENLOOP RESPONSE**

Steady state value (K) is calculated by applying a step input to the transfer function of the BW system. From the open loop response of the system steady state value K is obtained.

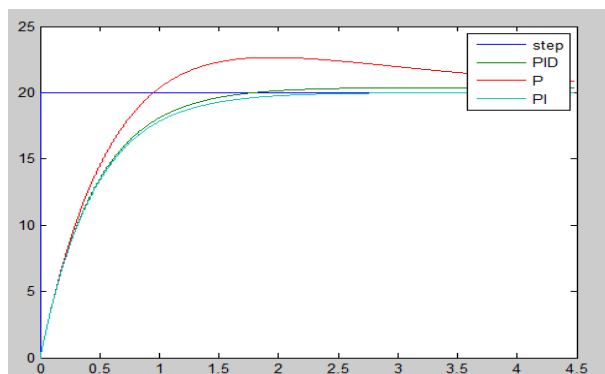


Fig 7: Closed loop response of current vs position





D) Choosing of Controllers

From the response graphs, the most appropriately signal following controllers with less overshoot, less offset, less oscillations are being choosed. While passing through the response graphs we can gaze the fact that PID controller holds good for pressure controlling and PI controller holds good for position controlling

E) Cascaded Controller

Cascade Control is an advanced application of the PID that can improve control of systems that are subject to significant lag. Since such systems are slow to respond to disturbances their performance can suffer with each upset. The Cascade architecture can be applied effectively to such sluggish processes when a related and faster responding loop is available. When applied in concert the faster loop serves as an early warning mechanism that buffers the impact on its slower counterpart, allowing for smoother control and

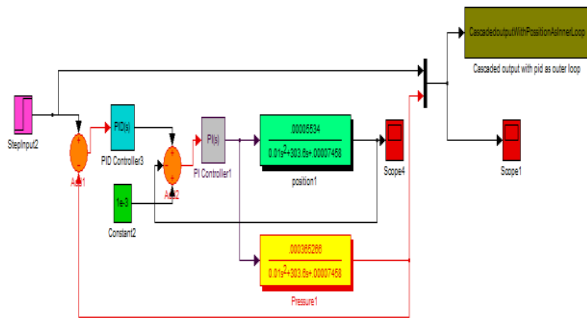


Fig 8: Simulink block diagram of cascade controller

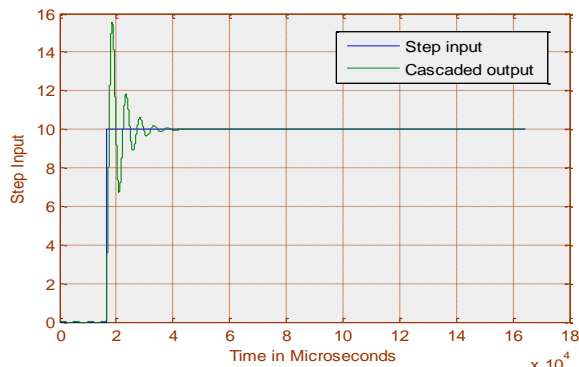


Fig 9: Closed loop response of the cascaded system.

From the response using the conventional PI and PID controllers on current to position and pressure to position controllers respectively high non linearities are occurring which should be suppressed. For reducing this non linearities proper tuning must be done. As the system contains high non linearity terms cascading controllers without turning is not advisable. Trial and error is a fundamental method of solving complicated problems. Even though the response of cascaded system seems to be settled with in short time period there occurred high oscillations which are not desirable in braking system. The increased oscillations should be suppressed, for that error

functions are calculated. Commonly used error functions are Mean Absolute Error and Mean Square Error.

$$ISE = \int_0^{\infty} \mathcal{E}^2 dt \tag{5}$$

$$IAE = \int_0^{\infty} |\mathcal{E}| dt \tag{6}$$

where  $\mathcal{E}$  is the error.

Mean square error and mean absolute error of the systems where calculated. The very next aim is to reduce the magnitude of these calculated errors, keeping in mind that the error signals removal will give better performance to the system. For achieving this optimisation techniques can be used. Here we used a harmonic search algorithm for reducing the mentioned two errors. Harmony search algorithm is an iterative technique for solving complicated turning process of higher order controller design. Using this algorithm we get the best value among the iterated values.

F) Fractional order controllers

Fractional-order control (FOC) is the field of control theory that uses the fractional-order integrator as part of the control system design toolkit. The fundamental advantage of FOC is that the fractional-order integrator weights history using a function that decays with a power-law tail. The effect is that the effects of all time are computed for each iteration of the control algorithm. This creates a 'distribution of time constants,' the upshot of which is there is no particular time constant, or resonance frequency, for the system. The transfer function of proportional controller is  $K_p$ .  $K_p$  is called the gain of the controller. The transfer function of PI controller is  $k_p \left( 1 + \frac{1}{T_i * s} \right)$ . The term  $K_p$  is the proportional gain and  $T_i$  is the integral time. The transfer function of proportional plus derivative controller is  $k_p (1 + T_d * s)$ . The term  $K_p$  is the proportional gain and  $T_d$  is the derivative time. The aim of using P-D controller is to increase the stability of the system by improving control since it has an ability to predict the future error of the system response The transfer function of a PID controller is  $k_p \left( 1 + T_d * s + \frac{1}{T_i * s} \right)$ . Here we have the constants in terms of unit power, where as in fractional order controller the power of these constants would be in fractional form. Likewise the power of all constants such as  $T_d, T_p, T_i$ , would be in fractional form. A PID controller is essentially a generic closed-loop feedback mechanism. Its working principle is that it monitors the error between a measured process variable and a desired set point; from this error, a corrective signal is computed and is eventually fed back to the input side to adjust the process accordingly. The differential equation of the PID controller is:

$$u(t) = K_p e(t) + T_i D^{-\lambda} e(t) + T_d D^{\delta} e(t) \tag{7}$$

Thus, the PID controller algorithm is described by a weighted sum of three time functions where the three



distinct weights are: the proportional gain ( $K_p$ ) that determines the influence of the present error-value on the control mechanism, the integral gain ( $T_i$ ) that decides the reaction based on the area under the error-time curve up to the present point and the derivative gain ( $T_d$ ) that accounts for the extent of the reaction to the rate of change of the error with time. Thus, the superposition of these three actions constitutes the mechanism for adjustment of plant performance.

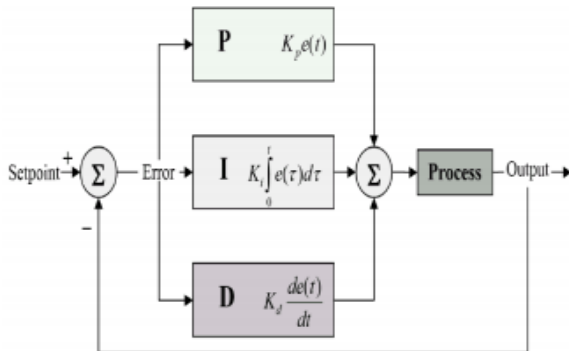


Fig 10: Generic closed loop control system with a PID controller

The differential equation of the  $PI^\lambda D^\delta$  controller is described by:

$$u(t) = K_p e(t) + T_i D^{-\lambda} e(t) + T_d D^\delta e(t) \quad (8)$$

The continuous transfer function of the  $PI^\lambda D^\delta$  controller is obtained through Laplace transform as:

$$G_c(s) = K_p + T_i s^{-\lambda} + T_d s^\delta \quad (9)$$

After the introduction of this definition, it is easily seen that classical types of PID controllers such as integral order PID, PI or PD become special cases of the most general fractional order PID controller. In other words, the  $PI^\lambda D^\delta$  controller expands the integer-order PID controller from point to plane, as shown in Fig. 10, thereby adding flexibility to controller design and allowing us to control our real world allowing us to control our real world processes more accurately but only at the cost of increased design complexity. This is, however, not at all a heavy price paid for the benefits obtained

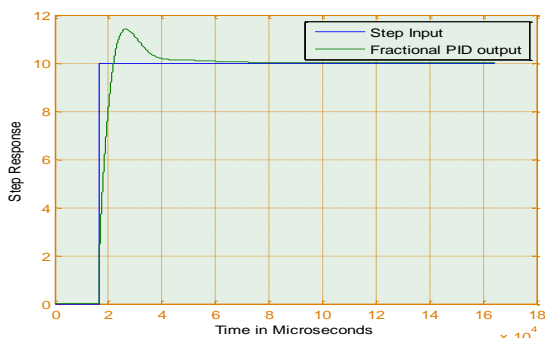


Fig11: Closed loop response of fractional order controller

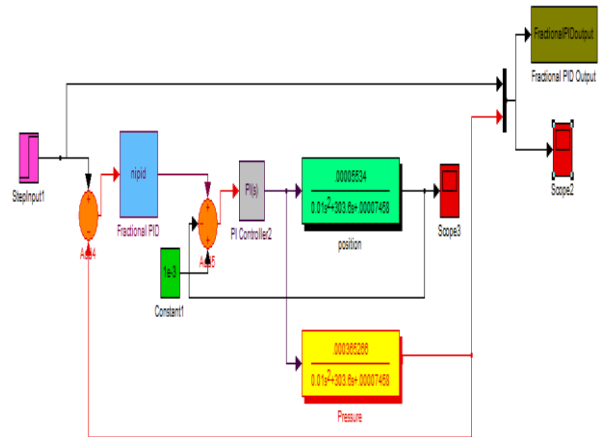


Fig 12: Simulink block diagram of Fractional Ordered Cascade Controller.

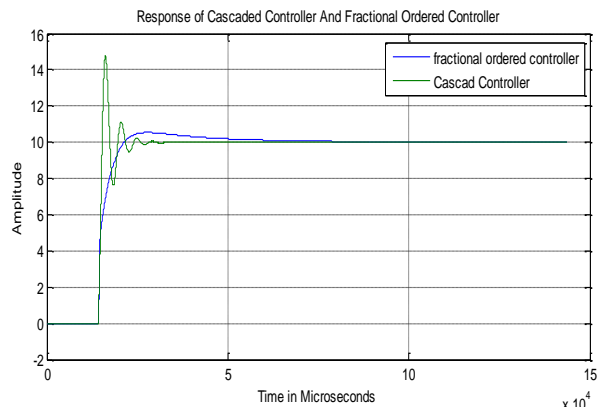


Fig 13: Response of Cascaded Controller and Fractional Ordered Controller

V. EXPERIMENTAL RESULTS

This section encompasses the experimental results. At first the choosed controllers where tested and they are cascaded. The responses are seems to be not ideal for a brake functioning. For rectifying the problem, presents of overshoot in the response should be minimised. For that the results error functions are plotted, then by means of harmonic search algorithm the error functions are minimised and there by fractional order controller where designed. Plots of both the cascaded controller and fractional order controller are compared.

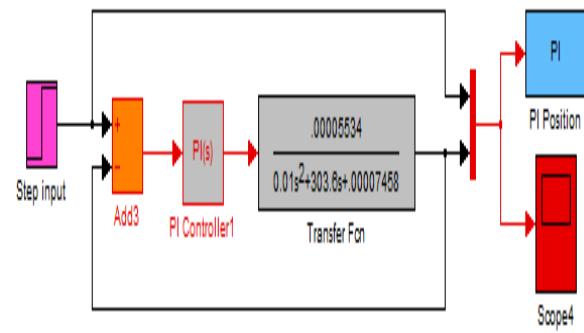


Fig 14: PI controller for current vs position

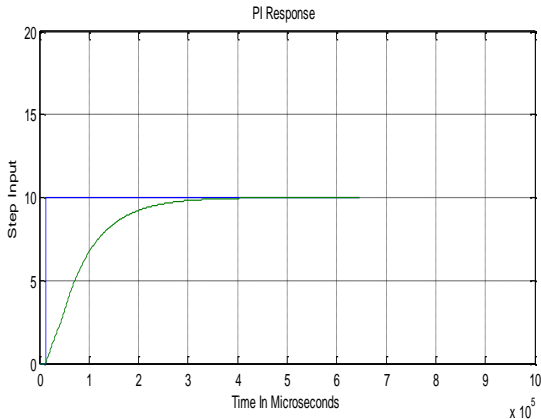


Fig 15: PI response for step input

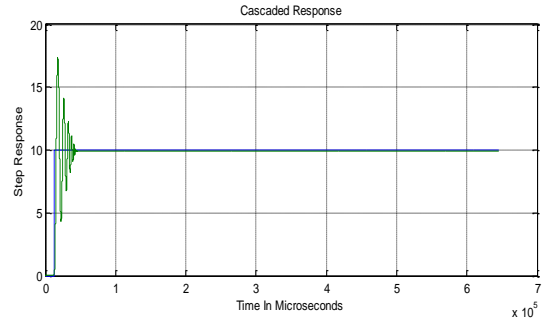


Fig 19: Cascaded response for step response

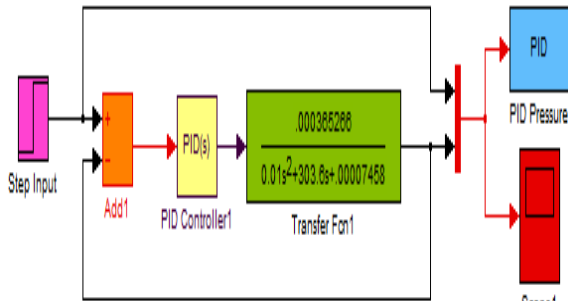


Fig 16: PID controller for current vs pressure

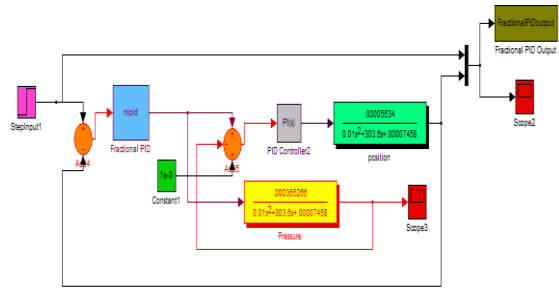


Fig 20: Fractional order controller

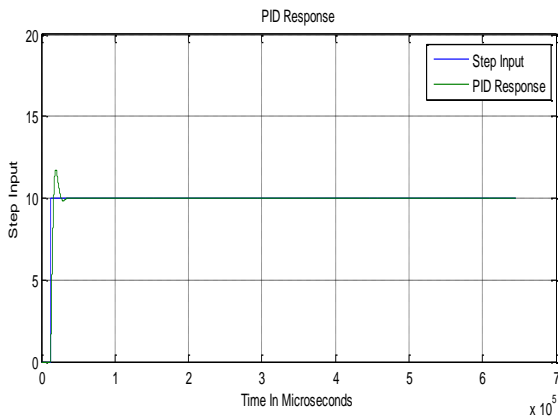


Fig 17: PID response for step response Cascading the controllers can be done in two ways.

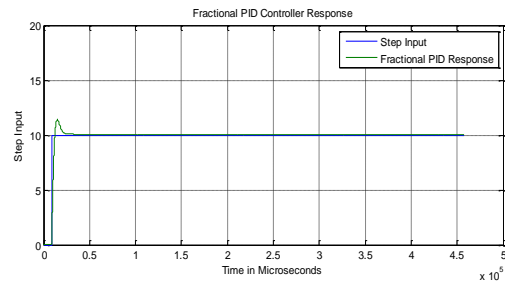


Fig 21: Response of Fractional order controller

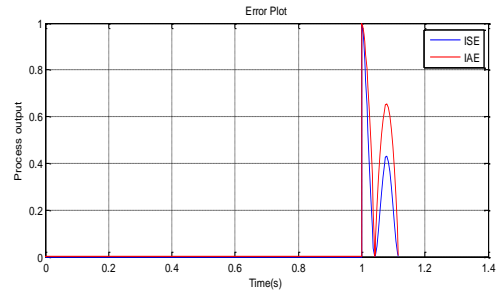


Fig 22: Integral Square Error and Integral Absolute Error of Cascaded Controller

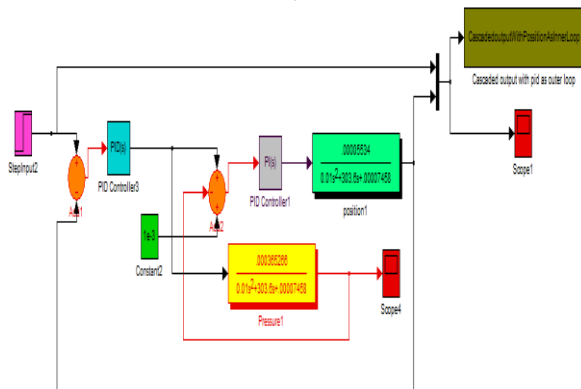


Fig 18: Cascaded controller (both PI and PID)

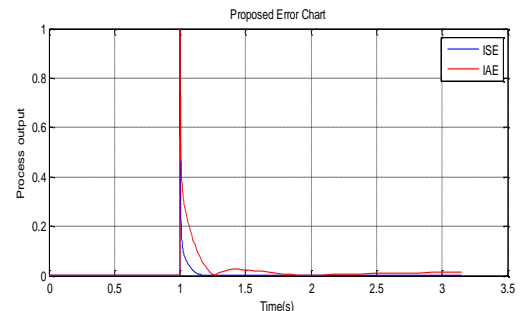


Fig 23: Integral Square Error and Integral Absolute Error of Fractional Order Controller



From the graph we can see that the fractional order controller's error is considerably low as considering with the cascaded controller. As the error in the response is minimised the controller is more prone to use than the previous one.

## VI. CONCLUSION

A robust controller which is capable for controlling a BBW actuator is presented. As proposed system consisting of a dead zone as well as an operative zone, two transfer functions where derived and for each transfer functions appropriate controllers where designed. The control architecture chosen is derived from the analysis of the control-oriented model. Notable thing is that, the transfer function between current and position exhibits an important propriety: above a certain frequency, the system is insensitive to the working point. Using this peculiarity, a cascade control is adopted: the inner loop is a position one, the outer loop a pressure one. Model identification as well as controller design are presented for both loops. The pressure controller aims to invert the intrinsic nonlinear position–pressure relationship since this nonlinear relationship is influenced by temperature and brake pad wear. The complete control architecture is thus a cascade control with a PI position controller and a PID fractional order pressure controller. This study highlighted that the combination of a normal PI and fractional order PID holds good response than that of a cascaded controller.

## REFERENCES

- [1] Fabio Todeschini, Matteo Corno, Giulio Panzani, Simone Fiorenti, and Sergio M. Savaresi, "Adaptive Cascade Control of a Brake-By-Wire Actuator for Sport Motorcycles", *Mechatronics*, vol. 20, No. 3, pp 1310-1319, 2015.
- [2] M. Tanelli, A. Astolfi, and S. Savaresi, "Robust nonlinear output feedback control for brake by wire control systems," *Automatica*, vol. 44, no. 4, pp. 1078–1087, 2008.
- [3] M. Tanelli, R. Sartori, and S. Savaresi, "Combining slip and deceleration control for brake-by-wire control systems: A sliding-mode approach." *Eur. J. Control*, vol. 13, no. 6, pp. 593–611, 2007.
- [4] M. Corno, S. Savaresi, and G. Balas, "On linear-parameter-varying (LPV) slip-controller design for two-wheeled vehicles," *Int. J. Robust Nonlinear Control*, vol. 19, no. 12, pp. 1313–1336, 2009.
- [5] M. Tanelli, M. Corno, I. Boniolo, and S. Savaresi, "Active braking control of two-wheeled vehicles on curves," *Int. J. Vehicle Auton. Syst.*, vol. 7, no. 3, pp. 243–269, 2009.
- [6] T. Johansen, I. Petersen, J. Kalkkuhl, and J. Ludemann, "Gain-scheduled wheel slip control in automotive brake systems," *IEEE Trans. Control Syst. Technol.*, vol. 11, no. 6 pp. 799–811, Nov. 811.
- [7] S. Savaresi, M. Tanelli, and C. Cantoni, "Mixed slip-deceleration control in automotive braking systems," *J. Dyn. Syst., Meas. Control*, vol. 129, pp. 20–31, 2007.
- [8] D. Reuter, E. Lloyd, J. Zehnder, and J. Elliott, "Hydraulic design considerations for EHB systems," presented at the SAE World Congr., MI, USA, 2003.
- [9] N. D'alfio, A. Morgando, and A. Sorniotti, "Electro-hydraulic brake systems: Design and test through hardware-in-the-loop simulation," *Vehicle Syst. Dyn, Int. J. Vehicle Mech. Mobility*, vol. 44, no. 1, pp. 378–392, 2006.
- [10] A. Sorniotti, and G. Repici, "Hardware in the loop with electro-hydraulic brake systems," presented at the 9th WSEAS Int. Conf. on Systems, Athens, Greece, 2005.
- [11] V. Milan'es, C. Gonz'alez, E. Naranjo, E. Onieva, and T. De Pedro, "Electrohydraulic braking system for autonomous vehicles," *Int. J. Automotive Technol.*, vol. 11, no. 1, pp. 89–95, 2010.
- [12] J. Kwak, B. Yao, and A. Bajaj, "Analytical model development and model reduction for electromechanical brake system," presented at the Int. Mechanical Engineering Congr. and Exp., Anaheim, CA, USA, 2004.
- [13] C. Line, "Modelling and control of an automotive electromechanical brake," Ph.D. Thesis, Univ. of Melbourne, Melbourne, Australia, 2007.
- [14] C. Rossa, A. Jaegy, J. Lozada, and A. Micaelli, "Design considerations for magnetorheological brakes," *IEEE/ASME Trans. Mechatronics*, vol. 19, no. 5 pp. 1669–1680, Oct. 1680.
- [15] H. Hartmann, M. Schautt, A. Pascucci, and B. Gombert, "ebrake R – the mechatronic wedge brake," in *Proc. SAE Conf. Proc. P. SAE*, 2002, pp. 15–20.
- [16] R. Roberts, M. Schautt, H. Hartmann, and B. Gombert, "Modelling and validation of the mechatronic wedge brake," *SAE paper*, vol. 112, pp. 2376–2386, 2003.
- [17] A. Dardanelli, G. Alli, and S. Savaresi, "Modeling and control of an electro-mechanical brake-by-wire actuator for a sport motorbike," the 5<sup>th</sup> IFAC Symp. Mechatronics Sys., Cambridge, MA, 2010, pp. 524–531.
- [18] G. Panzani, M. Corno, F. Todeschini, S. Fiorenti, and S. Savaresi, "Analysis and control of a brake by wire actuator for sport motorcycles," presented at the 13th Mechatronics Forum Int. Conf., Linz, Austria, Sep. 17–19, 2012.